Test Results of the LARP Nb_3Sn Quadrupole HQ03a

J. DiMarco, G. Ambrosio, M. Anerella, H. Bajas, G. Chlachidze, F. Borgnolutti, R. Bossert, D. Cheng, D. Dietderich, H. Felice, T. Holik, H. Pan, P. Ferracin, A. Ghosh, A. Godeke, A. R. Hafalia, M. Marchevsky, D. Orris, E. Ravaioli, G. Sabbi, T. Salmi, J. Schmalzle, S. Stoynev, T. Strauss, C. Sylvester, M. Tartaglia, E. Todesco, P. Wanderer, X. Wang, and M. Yu

***Abstract*—The U.S. LHC Accelerator Research Program (LARP) has been developing Nb_3Sn quadrupoles of increasing performance for the high-luminosity upgrade of the large hadron collider. The 120-mm aperture high-field quadrupole (HQ) models are the last step in the R&D phase supporting the development of the new IR Quadrupoles (MQXF). Three series of HQ coils were fabricated and assembled in a shell-based support structure, progressively optimizing the design and fabrication process. The final set of coils consistently applied the optimized design solutions and was assembled in the HQ03a model. This paper reports a summary of the HQ03a test results, including training, mechanical performance, field quality, and quench studies.**

***Index Terms*—High field accelerator magnets, Nb_3Sn.**

I. Introduction

THE HQ magnet is a 120 mm aperture, 1.5 meter long Nb_3Sn quadrupole developed by the LARP Program [1]. Its main goal is to provide a technology basis for the 150 mm aperture low-β quadrupoles (MQXF) that will be installed in the interaction regions of the High Luminosity LHC [2]. The first phase of the HQ program included production of eight coils, and five assembly cycles (HQ01a–HQ01e) [3]–[6]. These models, while demonstrating operation well above the HQ target gradient of 170 T/m, were affected by stress degradation, electrical insulation failures, and large dynamic field errors [7]–[10]. Detailed analysis [11] led to critical revisions of the coil parameters and components which were validated through dedicated tests in a mirror structure [12], [13] and gradually implemented in the HQ02 series [14]. The HQ02a model confirmed that the previous performance issues had been resolved, but its gradient was limited to 182 T/m due to the choice of a conservative pre-load level [15]–[17]. The next assembly, HQ02b, featured an increased pre-load and achieved a maximum gradient of 194 T/m at 1.9 K, corresponding to 94% of the short sample limit [18], [19]. In parallel, a third series of coils was fabricated to consistently apply the optimized design solutions, and improve the coil-to-coil uniformity [20]. The new coils (#22, #23, #24, and #26) were assembled in HQ03a, and two test cycles were performed at Fermilab in January 2015 and August-September 2015 (designated HQ03a and HQ03a2, respectively). The same coil and pre-load configuration was used in both cycles, but magnetic shims were introduced between cycles to test their effectiveness in correcting field errors. This paper presents a summary of the results, including quench history, mechanical performance and magnetic measurements.

TABLE I
HQ03 Conductor and Performance Parameters

Parameter	Unit	Value
Strand diameter	mm	0.778
Number of strands		35
Cable width	mm	15.002
Cable thickness	mm	1.44
Keystone angle	Deg.	0.75
Short sample current at 4.5K / 1.9K	kA	16.2 / 17.9
Short sample gradient at 4.5K / 1.9K	T/m	184 / 202

II. Design and Fabrication

HQ is a 1-meter long $\cos 2\theta$ quadrupole comprised of four double-layer coils assembled in a shell-based mechanical support structure. The design concept and main features are described in [3]–[6]. The conductor and performance parameters specific to the HQ03a assembly are summarized in Table I.

The superconducting cable, which incorporates a stainless steel core to control the dynamic effects, was fabricated as a single production unit using 0.778 mm diameter Nb_3Sn strands of the RRP 108/127 design [19]. A detailed report and analysis of the HQ03a coil design and fabrication is provided in [20]. As shown in Fig. 1, the four quadrants are assembled using bolted aluminum collars then aligned using keys inserted into each pole piece. The resulting coil pack is surrounded by bolted iron pads, inserted in a yoke-shell sub-assembly, and loaded using water-pressurized bladders and interference keys. Four tensioned aluminum rods are connected to stainless steel end plates to provide axial pre-load to the coils.

III. Quench Performance

The first test cycle of HQ03a at the Fermilab Vertical Magnet Test Facility (VMTF) was performed using a header assembly

Manuscript received October 19, 2015; accepted February 4, 2016. Date of publication March 9, 2016; date of current version May 11, 2016. This work was supported in part by the U.S. DOE Office of High Energy Physics under Contract DE-AC02-05CH11231.

J. DiMarco, G. Ambrosio, G. Chlachidze, R. Bossert, T. Holik, D. Orris, S. Stoynev, T. Strauss, C. Sylvester, M. Tartaglia, and M. Yu are with the Fermi National Accelerator Laboratory, Batavia, IL 60510 USA (e-mail: DiMarco@fnal.gov).

M. Anerella, A. Ghosh, J. Schmalzle, and P. Wanderer are with the Brookhaven National Laboratory, Upton, NY 11973 USA.

H. Bajas, P. Ferracin, E. Ravaioli, and E. Todesco are with the European Organization for Nuclear Research (CERN), 1211 Geneva, Switzerland.

F. Borgnolutti, D. Cheng, D. Dietderich, H. Felice, H. Pan, A. Godeke, A. R. Hafalia, M. Marchevsky, G. Sabbi, T. Salmi, and X. Wang are with the Lawrence Berkeley National Laboratory, Berkeley, CA 94720 USA.

Color versions of one or more of the figures in this paper are available online at http://ieeexplore.ieee.org.

Digital Object Identifier 10.1109/TASC.2016.2528283

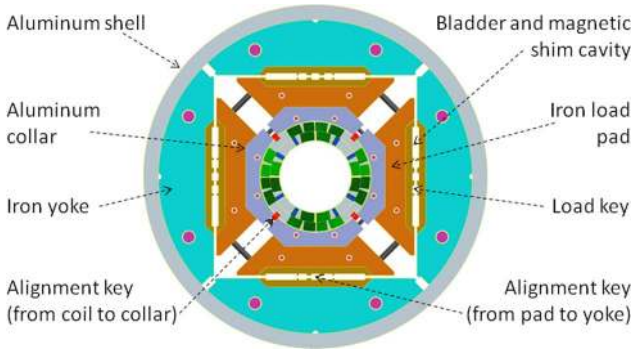

Fig. 1. LARP high field quadrupole (HQ) magnet cross-section.

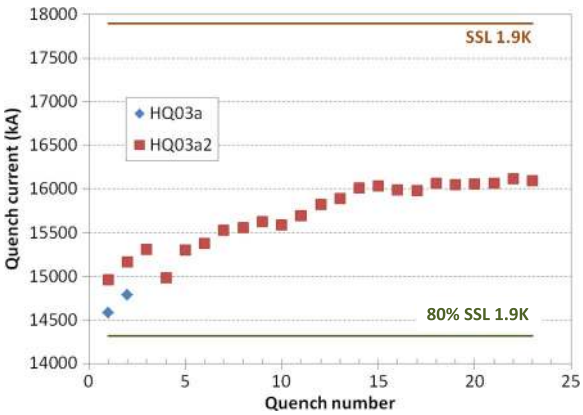

Fig. 2. Training history of HQ03a and HQ03a2 at 1.9 K compared to short sample limit (SSL) and nominal level (defined as 80% SSL).

rated for a maximum current of 15 kA. This limitation was removed in the HQ03a2 test, in which an upgraded header and configuration was rated for currents up to 30 kA. Both header assemblies were equipped with a lambda plate for testing magnets at superfluid helium temperatures.

Ten voltage taps were installed in both the inner and outer layers of each coil to help determine the locations where quenches originated. In addition, an inductive antenna based on a novel axial-field sensing technique [21] was installed in the magnet bore to characterize and optimize its performance for future use in full scale prototypes, where the increased coil length would make voltage taps less effective.

A. Quench Training

For both the HQ03a and the HQ03a2 test cycles, quench training was performed entirely at 1.9 K. The standard ramp rate at quench is 20 A/s, but a faster rate of 50 A/s is used in the first part of the ramp to reduce the turnaround time.

Fig. 2 shows the training history for both test cycles. HQ03a surpassed the nominal operating level (defined as 80% of the short sample limit) without quench, and reached the 15 kA maximum current allowed by the test setup, corresponding to 83.4% of the short sample limit, after two quenches. In the HQ03a2 cycle, the 15 kA performance level was recovered after a single training quench at 14.96 kA. Above 15 kA, the average rate of increase was about 60 A/quench, which was twice the rate of HQ02a in the same current range, but only a quarter

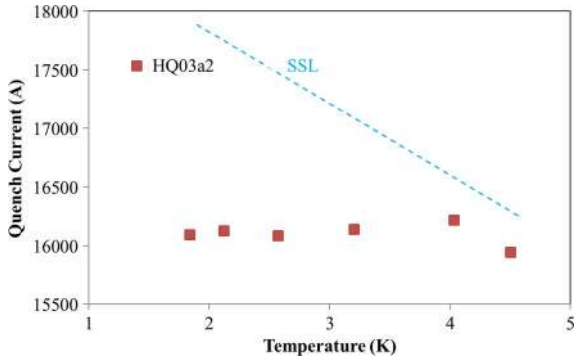

Fig. 3. Dependence of the quench current on temperature.

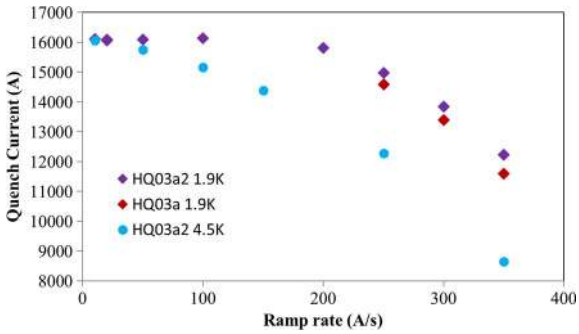

Fig. 4. Dependence of the quench current on ramp rate.

of HQ02b. After reaching 16 kA, progress became very slow and training was stopped after eight additional quenches. The highest current reached at 1.9 K was 16.1 kA or 90% of the short sample limit. Most training quenches were initiated in the inner layer pole-turn segments, and the remainder in the outer layer pole-turn segments.

In order to demonstrate stable performance at high current, the magnet was ramped to 14.3 kA (80% SSL) and maintained at this level for eight hours without quench.

B. Ramp Rate and Temperature Dependence Studies

A temperature dependence study was performed after training at 1.9 K (Fig. 3). No significant decrease of the quench current was observed up to 4 K, consistent with a mechanically limited plateau. At 4 K, a quench current of 16.22 kA was recorded, corresponding to 98% of the short sample limit. From 4 K to 4.5 K a 270 A reduction of the quench current was observed, consistent with the reduction of the conductor critical current in this temperature interval.

Fig. 4 shows the dependence of the quench current on ramp rate. At 1.9 K, no significant effect was observed up to 100 A/s, and the quenches originated at the pole turn, again indicating a mechanical origin of the quench plateau. From 200 A/s, a reduction of the quench current was observed and quenches originated in the mid-plane blocks of the inner and outer layer of coil 24, which has the lowest critical current based on extracted strand measurements. At 4.5 K, a monotonic reduction of the quench current with ramp rate was observed, consistent with a conductor limited quench level.

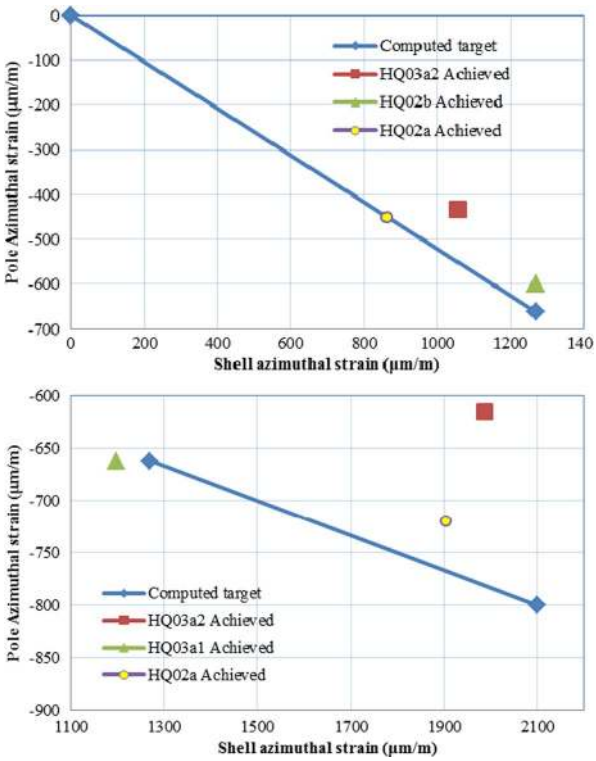

Fig. 5. Average strain measured at room temperature (upper plot), and after cool-down (lower plot) compared with the design targets.

The Residual Resistivity Ratio (RRR) measured during magnet warm-up was 130 in two of the quadrants (coils 22 and 26), and 110, 140 in the other two (coils 23 and 24). The RRR measurements were uniform across the segments of each coil, and the same values obtained in both thermal cycles.

IV. Mechanical Performance

The shell, coils and aluminum axial rods of the HQ03a magnet were instrumented with strain gauges: eight mounted on the aluminum shell (axial and azimuthal directions), four on the rods (axial) and eight on the coil titanium poles (axial and azimuthal directions). Their strain conditions were monitored during cool-down, training and warm-up.

Fig. 5 shows the measured average strain achieved for the shells and coil pole turns at warm and after cool-down, compared to the corresponding design targets. After cool-down, the average azimuthal strain on the shell was 1987 μm/m, reaching 94.6% of the computed target. The axial strain on rods reached about 98.7% of the target. The actual preloading on the pole turn at room temperature is about 19.4% lower than the target, and it becomes 23% lower at cold. These results indicate that insufficient pre-load is the cause of the slow rate of progress observed during training above 15 kA. Additional confirmation is provided by coil strain dependence on current. Fig. 6 shows the pole azimuthal strain as a function of current squared measured in the last training quench for coils 22, 24, and 26 (the strain gauges of coil 23 stopped functioning during the first test cycle). The non-linear response at high current indicates that all three coils are unloading, consistent with the observation that quenches started in all coils. Coil 26 unloads

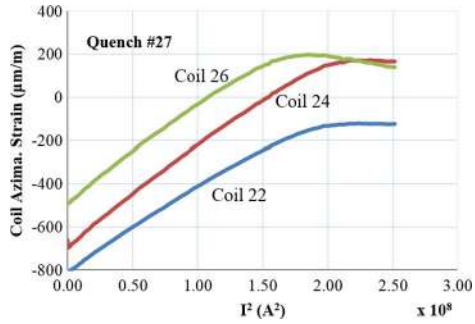

Fig. 6. Azimuthal strain of the pole vs. current squared at the end of training.

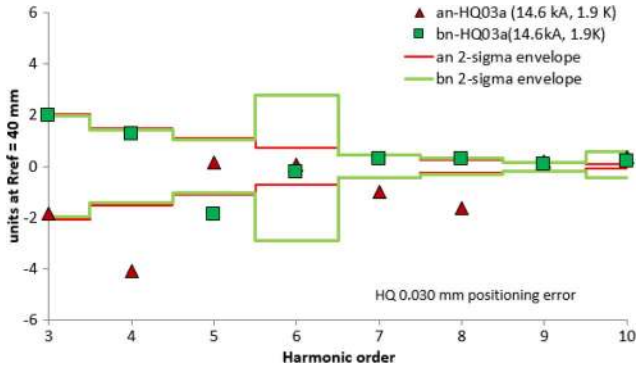

Fig. 7. Central harmonics at nominal gradient. The standard deviation is determined by a Monte Carlo simulation assuming ± 30 μm positioning tolerances for the conductor blocks.

first, around 12.5 kA, and coil 22–24 follow at a current of about 14 kA. Based on these results, an increase of the assembly pre-load is expected to improve the training rate and maximum quench level in future tests.

V. Magnetic Measurements

The magnetic field in the aperture of the quadrupole is expressed in terms of harmonic coefficients defined in a series expansion using the complex function formalism

$$B_y + iB_x = B_2 10^{-4} \sum_{n=1}^{\infty} (b_n + ia_n) \left(\frac{x+iy}{R_{\text{ref}}} \right)^{n-1} \qquad (1)$$

where B_x and B_y in (1) are the horizontal and vertical field components in the Cartesian coordinates, b_n and a_n are the $2n$-pole normal and skew harmonic coefficients at the reference radius $R_{\text{ref}} = 40$ mm.

Magnetic field measurements were performed utilizing the same coordinate and rotating coil probe systems as for HQ02 [16]. Fig. 7 shows the harmonic components measured at nominal gradient in the central straight section of HQ03a, compared with a Monte Carlo simulation using random displacements with a flat distribution of ± 30 μm. Several low order harmonics are larger than two standard deviations, indicating that the actual positioning errors are larger than 30 μm. In addition, the high order terms a_7 and a_8 are considerably larger in HQ03a than in previous models [16]. This effect is not compatible with a random fluctuation, but rather indicates a systematic deviation of a critical coil surface from its design position.

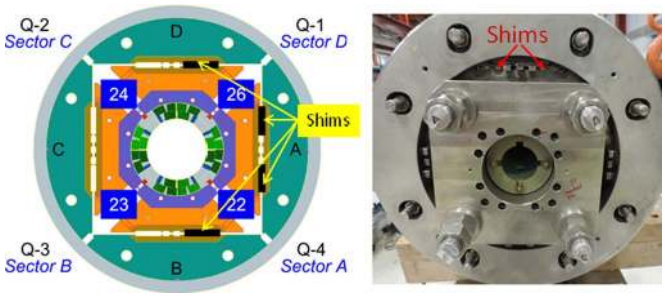

Fig. 8. Magnetic shim configuration in HQ03a.

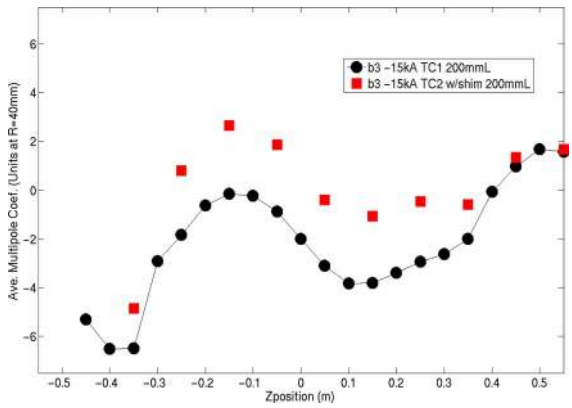

Fig. 9. Longitudinal scan of the normal sextupole in HQ03a (black) and HQ03a2 (red), showing the magnetic shim correction in the straight section.

Magnetic shims placed at the inner surface of the iron yoke have been shown to be an effective strategy to correct field errors [22], [23]. In the case of the MQXF quadrupoles, it has been proposed to place magnetic shims further inside the iron yoke, using the cavities provided to insert the pressurized bladders at assembly [24]. This technique was tested in HQ03a by inserting a set of magnetic shims between the two test cycles. The shims are designed to correct 2.5 units of the normal sextupole without changing the skew sextupole and the octupole components [25]. Fig. 8 shows the shim configuration, and Fig. 9 shows a comparison of the normal sextupole along the magnet length before and after correction.

While the intended correction was achieved within 10%, the large variations along the length are not corrected. In addition, this scheme fully utilizes the available tuning range, leaving no correction capability to be applied to other harmonics. Therefore, this magnetic shim implementation cannot fully substitute for improved accuracy and uniformity of the conductor positioning.

To estimate the effect of coupling currents on the magnet transfer function and the field quality, several excitation loops have been executed at ramp rates of 13 A/s, 20 A/s, 40 A/s, and 80 A/s. Figs. 10 and 11 show the measured variations of the quadrupole transfer function (TF) and normal dodecapole (b_6) as a function of the excitation current at different ramp rates. As in the case of HQ02, which also used cored cable, the HQ03a dependence on ramp rate is small. Fig. 12 shows that, in fact, the corresponding normal sextupole (b_3) has even smaller ramp rate dependence than in HQ02 [16], similar to what is

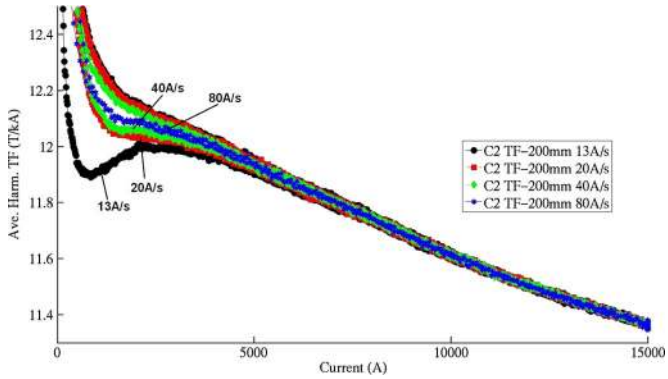

Fig. 10. Transfer function as a function of the magnet current at different ramp rates.

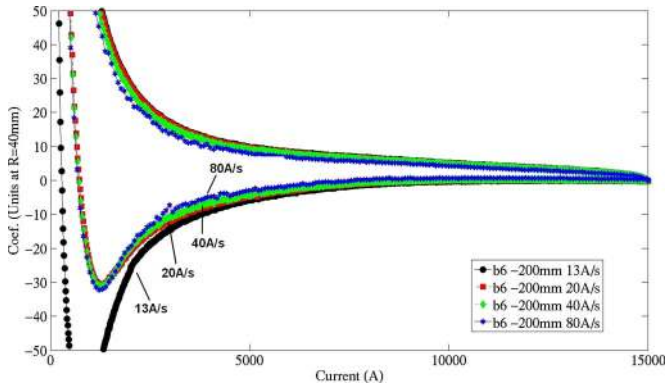

Fig. 11. Normal dodecapole as a function of the magnet current at different ramp rates.

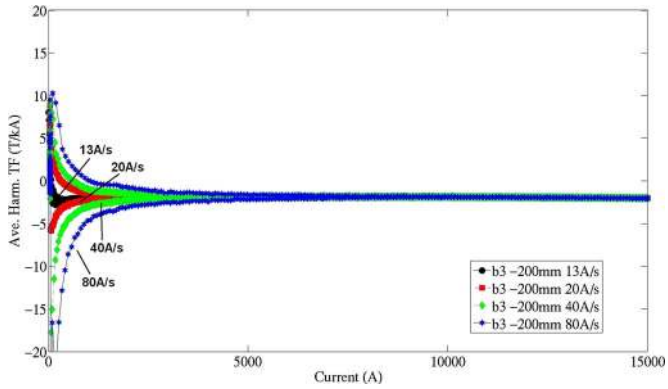

Fig. 12. Normal sextupole as a function of the magnet current at different ramp rates.

observed in the quench current. At the end of the ramp, these effects decay with a time constant of 4 s.

VI. Summary

The HQ03a model was successfully tested at the Fermilab Vertical Magnet Test Facility. The magnet reached 98% of the short sample limit at 4.5 K, confirming the validity of the optimized HQ coil design and fabrication process. A moderate increase of the pre-load is required to improve the training rate and approach the conductor limit at 1.9 K. The capability to apply an accurate field quality correction using magnetic shims was also demonstrated. However, in order to meet the stringent

field quality targets of future IR quadrupoles the accuracy and uniformity of the conductor positioning should be further improved relative to what has been achieved in HQ.

REFERENCES

[1] G. Sabbi, "Nb_3Sn IR quadrupoles for the high luminosity LHC," *IEEE Trans. Appl. Supercond.*, vol. 23, no. 3, Jun. 2013, Art. ID 4000707.

[2] O. Bruning and L. Rossi, Eds., "The high luminosity large hadron collider," in *Advanced Series on Directions in High Energy Physics*, vol. 24. Singapore: World Scientific, Oct. 2015.

[3] G. L. Sabbi *et al.*, "Design studies of Nb_3Sn high-gradient quadrupole models for LARP," *IEEE Trans. Appl. Supercond.*, vol. 17, no. 2, pp. 1051–1054, Jun. 2007.

[4] H. Felice *et al.*, "Magnetic and mechanical analysis of the HQ model quadrupole designs for LARP," *IEEE Trans. Appl. Supercond.*, vol. 18, no. 2, pp. 281–284, Jun. 2008.

[5] H. Felice *et al.*, "Design of HQ - a high field large bore Nb_3Sn quadrupole magnet for LARP," *IEEE Trans. Appl. Supercond.*, vol. 19, no. 3, pp. 1235–1239, Jun. 2009.

[6] S. Caspi *et al.*, "Design of a 120 mm bore 15 T quadrupole for the LHC upgrade phase II," *IEEE Trans. Appl. Supercond.*, vol. 20, no. 3, pp. 144–147, Jun. 2010.

[7] S. Caspi *et al.*, "Test results of 15 T Nb3Sn quadrupole magnet HQ01 with a 120 mm bore for the LHC luminosity upgrade," *IEEE Trans. Appl. Supercond.*, vol. 21, no. 3, pp. 1854–1857, Jun. 2011.

[8] P. Ferracin *et al.*, "Mechanical behavior of HQ01, a Nb_3Sn accelerator-quality quadrupole magnet for the LHC luminosity upgrade," *IEEE Trans. Appl. Supercond.*, vol. 22, no. 3, Jun. 2012, Art. ID 4901804.

[9] M. Marchevsky *et al.*, "Quench performance of HQ01, a 120 mm bore LARP quadrupole for the LHC upgrade," *IEEE Trans. Appl. Supercond.*, vol. 22, no. 3, Jun. 2012, Art. ID 4702005.

[10] H. Bajas *et al.*, "Cold test results of the LARP HQ Nb_3Sn quadrupole magnet at 1.9 K," *IEEE Trans. Appl. Supercond.*, vol. 23, no. 3, Jun. 2013, Art. ID 4002606.

[11] H. Felice *et al.*, "Impact of coil compaction on Nb_3Sn LARP HQ magnet," *IEEE Trans. Appl. Supercond.*, vol. 22, no. 3, Jun. 2012, Art. ID 4001904.

[12] R. Bossert *et al.*, "Optimization and test of 120 mm LARP Nb_3Sn quadrupole coils using magnetic mirror structure," *IEEE Trans. Appl. Supercond.*, vol. 22, no. 3, Jun. 2012, Art. ID 4003404.

[13] G. Chlachidze *et al.*, "Test of optimized 120-mm LARP Nb_3Sn quadrupole coil using magnetic mirror structure," *IEEE Trans. Appl. Supercond.*, vol. 23, no. 3, Jun. 2013, Art. ID 4001605

[14] F. Borgnolutti *et al.*, "Fabrication of a second-generation of Nb_3Sn coils for the LARP HQ02 quadrupole magnet," *IEEE Trans. Appl. Supercond.*, vol. 25, no. 3, Jun. 2014, Art. ID 4002505.

[15] G. Chlachidze *et al.*, "Performance of HQ02, an optimized version of the 120 mm Nb_3Sn LARP quadrupole," *IEEE Trans. Appl. Supercond.*, vol. 24, no. 3, Jun. 2014, Art. ID 4003805.

[16] J. DiMarco *et al.*, "Field quality measurements of LARP Nb_3Sn magnet HQ02," *IEEE Trans. Appl. Supercond.*, vol. 24, no. 3, Jun. 2014, Art. ID 4003905.

[17] X. Wang *et al.*, "Multipoles induced by inter-strand coupling currents in LARP Nb_3Sn quadrupoles," *IEEE Trans. Appl. Supercond.*, vol. 24, no. 3, Jun. 2014, Art. ID 4003905.

[18] H. Bajas *et al.*, "Test results of the LARP HQ02b magnet at 1.9 K," *IEEE Trans. Appl. Supercond.*, vol. 25, no. 3, Jun. 2015, Art. ID 4003306.

[19] A. Godeke *et al.*, "A review of conductor performance for the LARP high-gradient quadrupole magnets," *Supercond. Sci. Technol.*, vol. 26, no. 9, Aug. 2013, Art. ID 095015.

[20] F. Borgnolutti *et al.*, "Fabrication of a third generation of Nb_3Sn coils for the LARP HQ03 quadrupole magnet," *IEEE Trans. Appl. Supercond.*, vol. 25, no. 3, Jun. 2015. Art. ID 4002505.

[21] M. Marchevsky *et al.*, "Axial-field magnetic quench antenna for superconductor accelerator magnets," *IEEE Trans. Appl. Supercond.*, vol. 25, no. 3, Jun. 2015, Art. ID 9500605.

[22] R. Gupta, "Tuning shims for high field quality in superconducting magnets," *IEEE Trans. Magn.*, vol. 32, no. 4, pp. 2069–2073, Jul. 1996.

[23] G. Sabbi *et al.*, "Correction of high gradient quadrupole harmonics with magnetic shims," *IEEE Trans. Appl. Supercond.*, vol. 10, no. 1, pp. 123–126, Mar. 2000.

[24] P. Hagen, "Study of magnetic shimming in triplet magnets," Milestone Report 36 of HiLumi Design Study.

[25] X. Wang, J. DiMarco, and G. Sabbi, "Magnetic shim configuration for HQ03a magnet," HQ Technical Note, Feb. 19, 2015, LARP Doc 1077. [Online]. Available: https://larpdocs.fnal.gov/